ISSN: 2688-8645

A Miniaturized FBG Shape Sensor Based on a NiTi Substrate for Integration With Interventional Catheters

Lizhuang Sun [1], Weihan Zhang [2, 3], Zhangrui Yang [2, 3] and Yichao Tang [1, 4, *]

[1] School of Mechanical Engineering, Tongji University, Shanghai 200092, China

[2] Guohao College, Tongji University, Shanghai, China

[3] College of Electronic and Information Engineering, Tongji University, Shanghai 200092, China

[4] Shanghai Innovation Institute, Shanghai, 200433, China

* Corresponding author: Yichao Tang

Abstract

Three-dimensional catheter shape reconstruction is of considerable significance for minimally invasive cardiovascular navigation. This paper proposes a compact optical sensing scheme based on Fiber Bragg Gratings embedded in a NiTi-supported catheter structure. By combining strain-derived curvature estimation with Frenet-frame integration, the proposed method enables reconstruction of the catheter centerline from measured wavelength variations. The sensing structure is designed for improved compatibility with interventional catheter systems while maintaining a compact form factor. Static tests in planar and spatial bending configurations confirm that the reconstruction error remains within the millimeter range, demonstrating the practicality of the proposed approach.

Keywords

Fiber Bragg Gratings; NITI Substrate; Shape Sensing; Three-dimensional Reconstruction.

1. Introduction

Catheter-based intervention has become a standard approach for treating cardiovascular disease because it reduces surgical trauma and shortens postoperative recovery. Despite these advantages, the safety and effectiveness of such procedures still depend heavily on the operator's ability to perceive the catheter configuration inside complex vascular pathways. When the inserted catheter bends, deflects, or contacts the vessel wall, insufficient knowledge of its spatial shape may increase the risk of navigation error and unintended tissue interaction[1],[2],[3].

At present, intraoperative catheter guidance mainly relies on fluoroscopic imaging. Although fluoroscopy is routinely used in clinical interventions, it continuously exposes both the patient and the operator to ionizing radiation. In addition, the acquired images are essentially two-dimensional projections, which makes it difficult to directly recover the full three-dimensional geometry of the catheter in tortuous anatomical environments[4],[5],[6].

To overcome these limitations, fiber-optic sensing techniques have been increasingly investigated for catheter shape perception. Among them, Fiber Bragg Grating (FBG) sensors are especially attractive because they are lightweight, compact, highly sensitive to strain, and immune to electromagnetic interference. These characteristics make FBGs well suited to interventional devices operating in narrow and electromagnetically complex environments. Existing studies have shown that FBG-based sensing can provide effective geometric information for catheter or continuum-structure reconstruction. However, many reported sensing structures still face practical constraints in terms of miniaturization, assembly complexity, or compatibility with compact interventional catheters.

Motivated by these considerations, this paper develops a linearly arranged FBG shape sensor based on a slender NiTi substrate for integration with an interventional multi-lumen catheter. Three single-core optical fibers are distributed circumferentially to acquire deformation-induced wavelength variations, from which local curvature is estimated through a geometric model. The three-dimensional catheter centerline is then reconstructed using the Frenet frame. To assess the proposed method, calibration as well as planar and spatial bending experiments were carried out, followed by validation in a cardiovascular phantom. The results demonstrate that the proposed sensing strategy can provide a compact and feasible solution for catheter shape reconstruction in interventional applications.

2. Shape Sensing Model and Reconstruction Method

Three single-core optical fibers are arranged uniformly around the NiTi substrate with an angular spacing of 120°. During bending, the strain measured by each fiber is influenced by both the overall axial deformation of the structure and the bending effect associated with the fiber position. Based on this assumption, the strain of the *i*-th fiber can be described by Eq. (1), where the common term represents the average axial elongation of the cross-section and the remaining term accounts for bending relative to the neutral axis [7], [8].

$$\varepsilon_i(s) = k(s) r_i \cos(\theta_b - \theta_i) \tag{1}$$

Due to the symmetric distribution of the three sensing fibers, the shared axial strain component can be estimated by averaging the responses of all channels, as given in Eq. (2).

$$\varepsilon_A(s) = \frac{1}{N}\sum_{i=1}^{N} \varepsilon_i(s) \tag{2}$$

After removing this common component, the curvature components in the local cross-sectional frame can be obtained from the strain differences among the three fibers, leading to the relation expressed in Eq. (3). In this way, local bending information is directly extracted from the FBG responses.

$$k_x(s), k_y(s) \tag{3}$$

After the curvature distribution along the sensor is determined, the three-dimensional centerline is reconstructed through differential-geometric integration. In this work, the Frenet frame is adopted to describe the local evolution of the curve[9],[10]. The catheter centerline is parameterized by the arc-length variable *s*, and the tangent, normal, and binormal vectors evolve according to Eq. (4). Numerical integration of these quantities along the arc length yields the spatial shape of the catheter [11].

$$\begin{bmatrix} T^{'}(s) \\ N^{'}(s) \\ B^{'}(s) \end{bmatrix} = \begin{bmatrix} 0 & k(s) & 0 \\ -k_1(s) & 0 & \tau(s) \\ 0 & -\tau(s) & 0 \end{bmatrix} \begin{bmatrix} T(s) \\ N(s) \\ B(s) \end{bmatrix} \tag{4}$$

This method provides a practical reconstruction scheme for estimating the three-dimensional configuration of the catheter under bending-dominant deformation.

3. Sensor Fabrication and Assembly

This section presents the construction of the linear FBG shape sensor and its integration with the interventional catheter platform.

The sensing structure is formed by three single-core optical fibers mounted along the outer surface of a slender NiTi carrier, creating a compact sensing element for catheter shape measurement. The fibers are arranged circumferentially with a uniform angular separation of 120°. Each fiber incorporates three FBGs. The grating length is 10 mm, and the spacing between adjacent gratings is 40 mm, giving a total effective sensing length of 80 mm. FBG wavelength variations are recorded using an optical interrogator with a wavelength resolution of 0.1 pm and a sampling frequency of 30 Hz.

The NiTi carrier functions as the supporting substrate of the sensing unit. To position the optical fibers, longitudinal grooves are fabricated on the substrate surface, and the fibers are fixed in place using EPO-TEK 353ND adhesive so that deformation of the substrate can be transferred effectively to the gratings. After the fiber assembly is completed, the sensing unit is combined with a five-lumen PEBAX catheter for interventional use. The catheter contains a central lumen for tool delivery and several peripheral lumens reserved for actuation wires, allowing the catheter to maintain its operational functionality while incorporating shape sensing capability.

Compared with sensing structures that rely on bulkier carriers or more elaborate packaging strategies, the present NiTi-based configuration features a more compact form and is better suited for integration with narrow interventional instruments.

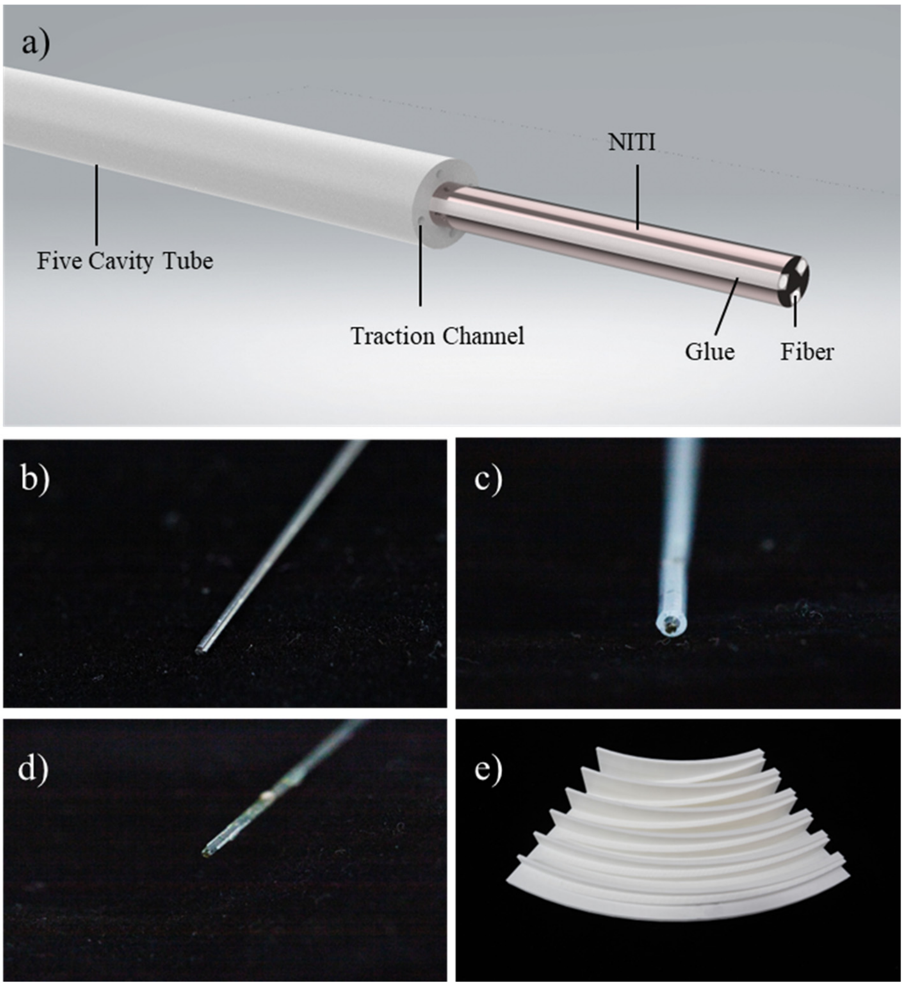

Fig 1. Fabrication of the NiTi-substrate linear FBG shape sensor and calibration molds.(a) Schematic illustration of the sensor structure integrated with a five-cavity catheter, showing the NiTi substrate, optical fibers, adhesive layer, and traction channels;(b) photograph of the grooved NiTi substrate;(c) end-view photograph of the NiTi substrate cross-section;(d) photograph of the fabricated FBG sensor after fiber bonding;(e) 3D-printed calibration molds used for constant-curvature bending tests.

4. Results and Discussion

To examine the performance of the proposed sensing strategy, several static experiments were carried out, including calibration, planar and three-dimensional bending evaluation, and validation in a branched cardiovascular phantom.

4.1 Calibration

Prior to shape reconstruction, a calibration procedure was performed to determine the correspondence between FBG wavelength variation and known curvature input, while also compensating for channel inconsistency introduced during sensor fabrication and assembly, as shown in figure 2. The sensor was first maintained in its undeformed straight configuration, and the initial wavelengths of all gratings were taken as baseline values. It was then successively constrained in circular molds of known radii to produce constant-curvature bending. The wavelength responses obtained under these prescribed conditions were used to calculate the calibration coefficients employed in the subsequent reconstruction process.

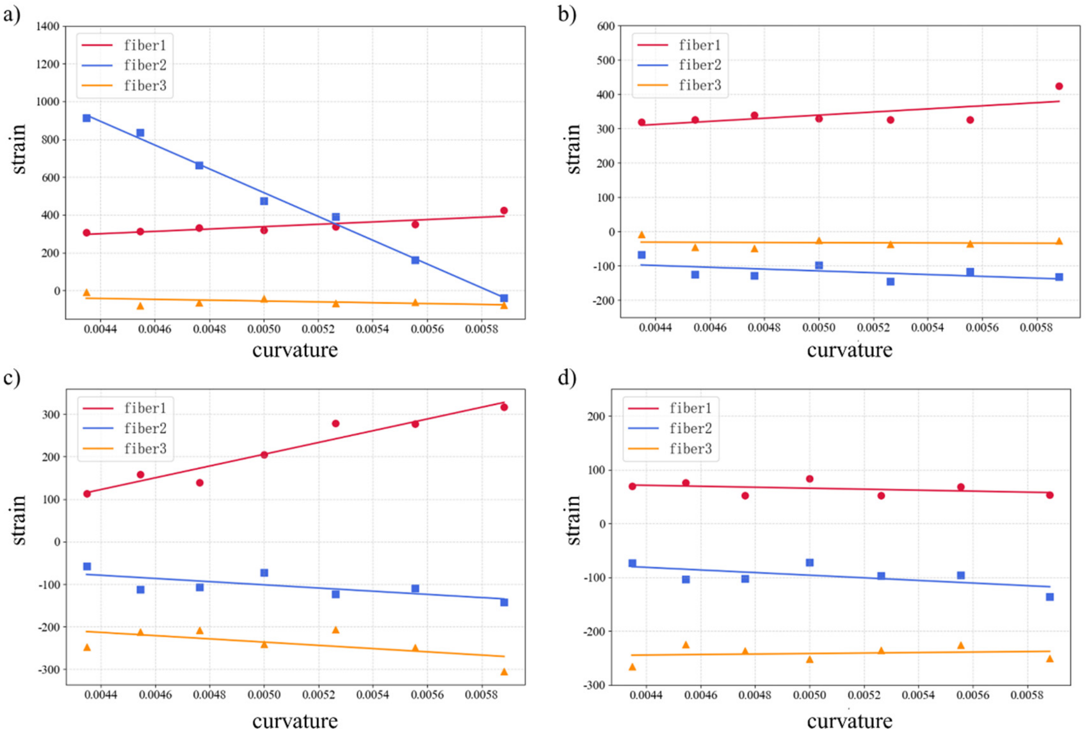

Fig 2. Strain calibration results of the three sensing fibers at four representative cross-sections. (a)–(d) Calibration data obtained from different FBG groups under constant-curvature loading, showing the relationship between measured strain and applied curvature for fiber 1, fiber 2, and fiber 3.

4.2 Planar and Spatial Bending Accuracy

The reconstruction capability of the sensor was evaluated using high-precision 3D-printed molds designed for both planar and spatial bending conditions. For the planar tests, the mold radii ranged from 150 mm to 210 mm. The spatial cases were generated using molds with different three-dimensional geometric parameters. All molds were fabricated with dimensional tolerances within ±0.1 mm.

In each experiment, the sensor was fitted to the target mold so that repeatable deformation could be imposed. The measured FBG responses were then converted into curvature and used to reconstruct the catheter centerline. Reconstruction performance was quantified by the rootmean-square error (RMSE) and the pointwise deviation along the arc length, the data is shown in Table 1.

As shown in figure 3, The reconstructed curves show good agreement with the reference geometries under both types of loading. For planar bending, the overall error remains within the millimeter range over the tested curvature conditions. In the spatial cases, the reconstruction deviation becomes moderately larger, which can be attributed to the increased geometric complexity of out-of-plane deformation. Even so, the reconstructed centerlines still closely match the corresponding reference shapes, indicating that the proposed method maintains stable reconstruction performance in both planar and spatial bending scenarios.

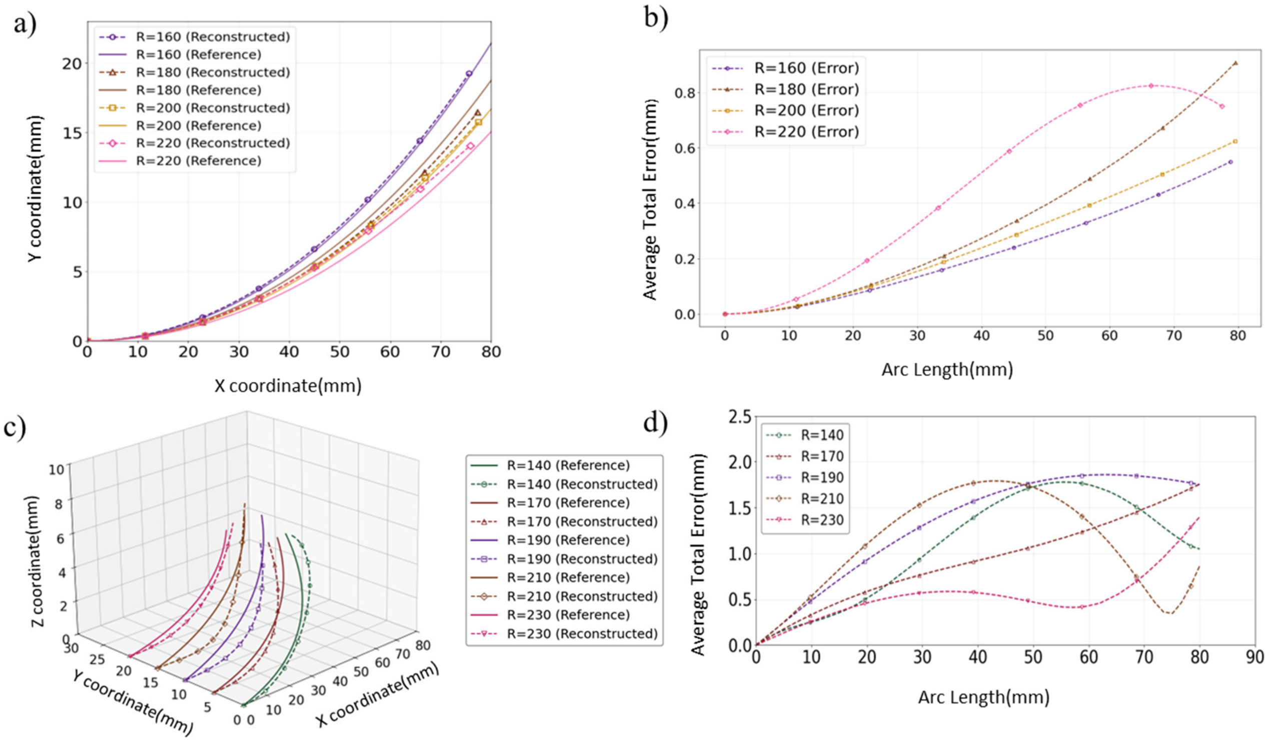

Fig 3. Accuracy assessment of the reconstructed catheter shapes under planar and spatial bending conditions.(a) Comparison between reconstructed and reference centerlines for planar bending with different curvature radii;(b) pointwise reconstruction errors along the arc length for the planar cases;(c) comparison between reconstructed and reference centerlines for representative three-dimensional bending configurations;(d) arc-length-wise error distributions for the spatial cases.

Table 1. Reconstruction Errors under Different Configurations

Config		R160	R170	R180	R190	R200	R210
2D	$r_e\,(mm)$	0.55	1.27	0.94	1.21	0.61	0.89
	$r_{RMSE}\,(mm)$	0.35	0.51	0.49	0.67	0.58	0.66
3D	$r_e\,(mm)$	1.45	1.76	1.89	1.83	1.55	1.78
	$r_{RMSE}\,(mm)$	0.94	0.87	1.02	1.24	1.07	0.93

5. Conclusion

This study developed a compact FBG-based shape sensor using a NiTi substrate for interventional catheter integration. By combining symmetric fiber arrangement, strain-based curvature estimation, and Frenet-frame reconstruction, the proposed method enables three-dimensional catheter shape recovery. The experimental results demonstrate millimeter-level accuracy in planar and spatial bending tests, and phantom validation further confirms its feasibility in complex pathways. These findings indicate that the proposed sensor provides a practical solution for catheter shape sensing, with future work directed toward dynamic evaluation and further application-oriented optimization.

References

[1] C. Zhou, Z. Lin, S. Huang, B. Li, and A. Gao, “Progress in Probe-Based Sensing Techniques for In Vivo Diagnosis,” Biosensors, vol. 12, no. 11, p. 943, Oct. 2022.

[2] A. Ali, D. Plettenburg, and P. Breedveld, “Steerable Catheters in Cardiology: Classifying Steerability and Assessing Future Challenges,” IEEE Trans. Biomed. Eng., pp. 1–1, 2016, doi: 10.1109/ TBME. 2016.2525785.

[3] Z. Lin et al., “ARei: Augmented-Reality-Assisted Touchless Teleoperated Robot for Endoluminal Intervention,” IEEEASME Trans. Mechatron., vol. 27, no. 5, pp. 3144–3154, Oct. 2022.

[4] Z. Lin et al., “Fixed and Sliding FBG Sensors-Based Triaxial Tip Force Sensing for Cable-Driven Continuum Robots,” in 2022 International Conference on Robotics and Automation (ICRA), Philadelphia, PA, USA: IEEE, May 2022, pp. 9593–9599.

[5] X. T. Ha, D. Wu, M. Ourak, G. Borghesan, A. Menciassi, and E. V. Poorten, “Sensor Fusion for Shape Reconstruction Using Electromagnetic Tracking Sensors and Multi-Core Optical Fiber,” IEEE Robot. Autom. Lett., vol. 8, no. 7, pp. 4076–4083, July 2023.

[6] X. T. Ha et al., “Robust Catheter Tracking by Fusing Electromagnetic Tracking, Fiber Bragg Grating and Sparse Fluoroscopic Images,” IEEE Sensors J., vol. 21, no. 20, pp. 23422–23434, Oct. 2021, doi: 10.1109/JSEN.2021.3107036.

[7] Y. Lu et al., “Autonomous Intelligent Navigation for Flexible Endoscopy Using Monocular Depth Guidance and 3-D Shape Planning,” in 2023 IEEE International Conference on Robotics and Automation (ICRA), London, United Kingdom: IEEE, May 2023, pp. 1–7. doi: 10.1109/ ICRA48891. 2023. 10161505.

[8] J. P. Moore and M. D. Rogge, “Shape sensing using multi-core fiber optic cable and parametric curve solutions,” Opt. Express, vol. 20, no. 3, p. 2967, Jan. 2012.

[9] G. Robinson and J. B. C. Davies, “Continuum robots - a state of the art,” in Proceedings 1999 IEEE International Conference on Robotics and Automation (Cat. No.99CH36288C), Detroit, MI, USA: IEEE, 1999, pp. 2849–2854.

[10] D. Carroll, E. Köse, and I. Sterling, “Improving Frenet’s frame using Bishop’s frame,” J. Math. Res., vol. 5, no. 4, pp. 97–106, Nov. 2013.

[11] J. Langer and D. A. Singer, “Lagrangian aspects of the Kirchhoff elastic rod,” SIAM Rev., vol. 38, no. 4, pp. 605–618, Dec. 1996.